

2015

Confocal fluorescence microscopy: An ultra-sensitive tool used to evaluate intracellular antiretroviral nano-drug delivery in HeLa cells

Subhra Mandal

Creighton University, SubhraMandal@creighton.edu

You Zhou

University of Nebraska-Lincoln, yzhou2@unl.edu


Annemarie Shibata

Creighton University

Christopher J. Destache

Creighton University, cjd42123@creighton.edu

Follow this and additional works at: <http://digitalcommons.unl.edu/vetscipayers>

 Part of the [Biochemistry, Biophysics, and Structural Biology Commons](#), [Cell and Developmental Biology Commons](#), [Immunology and Infectious Disease Commons](#), [Medical Sciences Commons](#), [Veterinary Microbiology and Immunobiology Commons](#), and the [Veterinary Pathology and Pathobiology Commons](#)

Mandal, Subhra; Zhou, You; Shibata, Annemarie; and Destache, Christopher J., "Confocal fluorescence microscopy: An ultra-sensitive tool used to evaluate intracellular antiretroviral nano-drug delivery in HeLa cells" (2015). *Papers in Veterinary and Biomedical Science*. 170.

<http://digitalcommons.unl.edu/vetscipayers/170>

This Article is brought to you for free and open access by the Veterinary and Biomedical Sciences, Department of at DigitalCommons@University of Nebraska - Lincoln. It has been accepted for inclusion in Papers in Veterinary and Biomedical Science by an authorized administrator of DigitalCommons@University of Nebraska - Lincoln.

Confocal fluorescence microscopy: An ultra-sensitive tool used to evaluate intracellular antiretroviral nano-drug delivery in HeLa cells

Subhra Mandal,^{1,a} You Zhou,² Annemarie Shibata,³ and Christopher J. Destache¹

¹*School of Pharmacy and Health Professions, Creighton University, Omaha, NE 68178, USA*

²*Center for Biotechnology, the University of Nebraska-Lincoln, Lincoln, NE 68588, USA*

³*Department of Biology, Creighton University, Omaha, NE 68178, USA*

(Received 10 May 2015; accepted 29 June 2015; published online 8 July 2015)

In the last decade, confocal fluorescence microscopy has emerged as an ultra-sensitive tool for real-time study of nanoparticles (NPs) fate at the cellular-level. According to WHO 2007 report, Human Immunodeficiency Virus/Acquired Immunodeficiency Syndrome (HIV/AIDS) is still one of the world's major health threats by claiming approximately 7,000 new infections daily worldwide. Although combination antiretroviral drugs (cARV) therapy has improved the life-expectancy of HIV-infected patients, routine use of high doses of cARV has serious health consequences and requires complete adherence to the regimen for success. Thus, our research goal is to fabricate long-acting novel cARV loaded poly(lactide-co-glycolic acid) (PLGA) nanoparticles (cARV-NPs) as drug delivery system. However, important aspects of cARV-NPs that require special emphasis are their cellular-uptake, potency, and sustained drug release efficiency over-time. In this article, ultra-sensitive confocal microscopy is been used to evaluate the uptake and sustained drug release kinetics of cARV-NPs in HeLa cells. To evaluate with the above goal, instead of cARV-drug, Rhodamine6G dye (fluorescent dye) loaded NPs (Rho6G NPs) have been formulated. To correlate the Rhodamine6G release kinetics with the ARV release from NPs, a parallel HPLC study was also performed. The results obtained indicate that Rho6G NPs were efficiently taken up at low concentration (<500 ng/ml) and that release was sustained for a minimum of 4 days of treatment. Therefore, high drug assimilation and sustained release properties of PLGA-NPs make them an attractive vehicle for cARV nano-drug delivery with the potential to reduce drug dosage as well as the number of drug administrations per month. © 2015 Author(s). All article content, except where otherwise noted, is licensed under a Creative Commons Attribution 3.0 Unported License. [<http://dx.doi.org/10.1063/1.4926584>]

INTRODUCTION

Fluorescence microscopy has advanced cell biology dramatically, mainly by revolutionizing the cellular uptake studies.¹ Confocal fluorescence imaging has emerged as one of the basic techniques used in the field of nano-drug delivery system to study in real-time cellular uptake and sustainability of NPs contents over time.²

Human Immunodeficiency Virus/Acquired Immunodeficiency Syndrome (HIV/AIDS) is a major health threat to the human population. According to World Health Organization (WHO) 2007 estimation, for each person that receives treatment with antiretroviral (ARV) drugs, four newly HIV-infected persons are reported.³ In the last three decades, tremendous effort has been put forth to develop new drugs to treat and/or prevent HIV infection. Among them, combined antiretroviral therapy (cART)⁴

^aCorrespondence to: S. Mandal, Department of Pharmacy Practice, School of Pharmacy and Health Professions, Creighton University, Omaha, NE 68178, USA. Email: subhramandal@gmail.com; SubhraMandal@creighton.edu



has generated new hope by reducing HIV-1 replication and lowering viral load (VL) to an undetectable level in the patient's plasma. The cART mainly involves the use of three or more combinations of ARV drugs (cARV) to block different stages of HIV replication. Although, cART has shown reduction in VL, there is serious health issues associated with cART use. These issues includes, >95 % patient adherence for success, significant physiological side effects, and ineffectiveness against viral bio-reservoirs.⁵⁻⁷ The major physicochemical drawbacks of cARV drugs are their hydrophobicity, poor tissue penetrance, and short-systemic retention time. Therefore, to maintain a considerable amount of these cARV drugs in the patient's blood to reduce VL to an undetectable level, these cARV drugs are administered in large amounts on a daily basis. Failure to take daily doses can lead to the development of resistance or reduce efficacy of cART, leading to elevation of VL in patients' blood and reductions in CD4 T-helper lymphocytes.

Nanoparticles (NPs) are emerging as a very promising tool as cARV-drug delivery system primarily due to their prolong stability, improve adherence and sustained-drug release potentials. The sustained-release property of NP would potentially result in reduction of ARV drug administrations (both in frequency and amount), and in turn shall ensure long term non-detectable VL in the patient's blood. Among various synthetic polymers, poly(lactide-co-glycolic acid) (PLGA), a Food and Drug Administration (FDA) approved polymer, is extensively exploited to develop NPs (PLGA NPs) due to their properties like biocompatible, biodegradable, and exhibit long term systemic and physical storage stability.⁸

Our research goal is to fabricate PLGA NP based cARV nano-drug delivery systems to overcome cART drawbacks. We have already demonstrated that a single intraperitoneal (ip) injection of NPs containing ARV drugs (cARV NPs) results in sustained *in vivo* release of antiretroviral drugs in mice.⁹ Interestingly, we observed high levels of ARV drugs in HIV reservoirs such as the brain, liver, spleen, kidney, and testes for a period of 28 days whereas antiretroviral drug solutions showed detectable drug levels for only 48–72 h.⁹

The biological consequences of NPs at the cellular level, namely their uptake, sustenance in the cellular organelles, and drug release pattern need to be thoroughly investigated prior to translation to animal and then to the clinical studies. However, among various studies the most important aspect is to determine the fate of cARV NPs at the endothelial membrane, the primary barrier that NPs encounter before reaching their target. Therefore, a comprehensive study at the cellular level is very important to understand the ARV NPs uptake mechanism, their retention time, and pharmacokinetics.

Primarily, NPs enter in the cells via endocytosis.¹⁰ The principal characteristic of NPs influencing their cellular uptake is their size equivalence with that of subcellular components. Other than size of NPs, surface charge and compatibility with the targeted cell type also influences their cellular uptake mechanism.^{11,12} The ability to tag/label fluorescence molecules with NPs enables their real-time tracking at the cellular level using confocal fluorescence microscopy. Therefore, for the present work, we formulated Rhodamine 6G dye (Rho6G) PLGA NPs (Rho6G NPs) and/ Rilpivirine (RPV) (ARV drug) loaded PLGA NPs (RPV/Rho6G NPs), to visualize them under the confocal fluorescence microscope. Confocal fluorescence microscopic imaging was performed to study in real-time NP uptake, sustainability, and drug release kinetics in HeLa cells. However, to correlate Rho6G release profile from NPs with ARV drug release, we performed HPLC study to evaluate the correlation between Rho6G dye and RPV drug release from RPV/Rho6G NPs in the HeLa cells. Our present study demonstrates that the use of confocal fluorescent microscopy has enabled us to evaluate ARV drug release property of PLGA NPs. Given our results, we propose that PLGA NPs as a drug delivery system has the potential to overcome the deficiencies of present day cART and to improve the life of HIV-positive patients.

MATERIALS AND METHODS

Materials

PLGA (75:25 lactide:glycolide ratio; Mw 4,000-15,000), Poly(vinyl alcohol) (PVA) (M.W. 13,000–23,000), Dichloromethane (DCM), Acetonitrile (ACN), Potassium dihydrogen phosphate (KH₂PO₄), Mowiol 4-88 and Phosphate Buffered Saline (PBS) were purchased from Sigma-Aldrich

(St. Louis, MO, USA). Pluronic F127 (PF-127), Rilpivirine (RPV; 99% purity), Rhodamine 6G dye (Rho6G; 99% purity) were from purchased from D-BASF (Edinburgh, UK), Sequoia Research Products Ltd (Pangbourne, RG8 7AP, UK) and Acros Organics (NJ, USA), respectively. The 3,3'-Diocetadecyl-5,5'-Di(4-Sulfophenyl)Oxycarbocyanine (DiO) dye, and Hoechst 33342 dye were purchased from Life Technologies (Eugene, OR, USA). Dimethyl Sulfoxide (DMSO), Paraformaldehyde (PFA) and Acetonitrile were purchased from Fisher BioReagents and Fisher Chemicals (Fair Lawn, NJ, USA). Roswell Park Memorial Institute medium 1640 (RPMI-1640), Fetal Bovine Serum (FBS), L-Glutamine, Trypsin and Penicillin-Streptomycin (Penstep) Solution were purchased from Hyclone™ (Logan, Utah, USA). All reagents were used as received without further purification.

PLGA NPs formulation and characterization

PLGA NPs were prepared by interfacial polymer deposition method¹³ as described in **Figure 1**.¹⁴ Briefly, 100 mg of PLGA was dissolved in the 2.5 mL DCM (the organic phase) containing PF-127 as stabilizer. To formulate Rho6G loaded PLGA NPs (Rho6G NPs), Rho6G (5 mg) was added to the above organic phase, whereas to formulation RPV and Rho6G loaded PLGA NPs (RPV/Rho6G NPs), RPV (5 mg) and Rho6G (1 mg) were added sequentially under constant magnetic stirring. The above organic phase was added to 10ml of 1 % PVA solution (aqueous phase). The above oil-in-water (o/w) emulsion was sonicated for 5 min. The organic phase was eliminated by evaporation. Finally, the surfactants, free RPV and Rho6G were washed off from NPs by three times washing with MQ water (18.2 MΩ), by centrifugation at 14, 000Xg for 20 min. The NPs thus obtained were freeze-dried in the Millrock LD85 lyophilizer (Kingston,NY, USA).

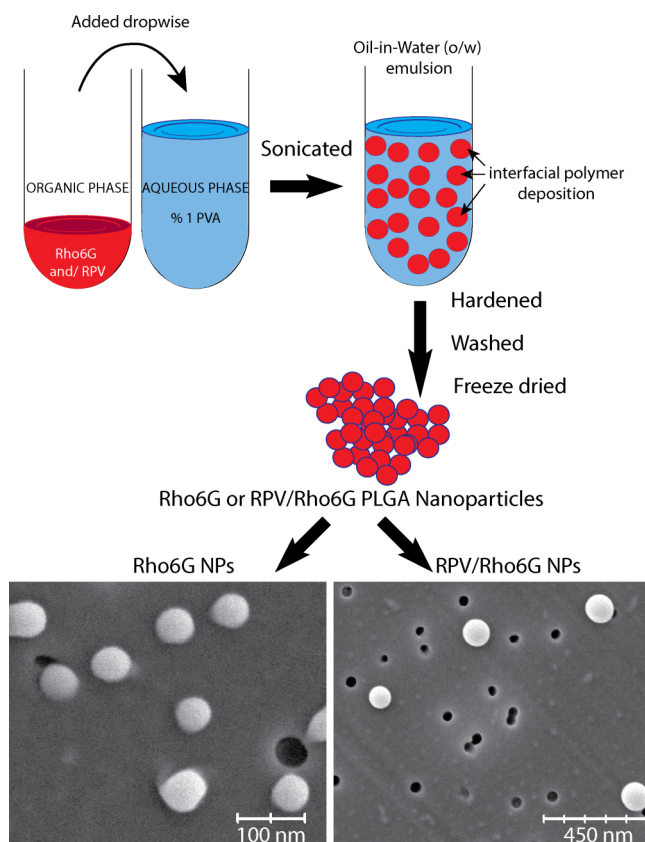


FIG. 1. PLGA NP formulation by interfacial polymer deposition method. First part of the figure schematically describes stepwise the nanoparticle preparation method. Below SEM images are representative image of the Rho6G NPs (left) and RPV/Rho6G NPs (right).

An appropriate amount of freeze-dried RPV NPs and RPV/Rho6G NPs were dispersed in MQ water at room temperature (RT) for their characterization. The size, polydispersity index (PDI) and zeta potential of the NPs were characterized by using the ZetaPlus Zeta Potential Analyzer (Brookhaven Instruments Corporation, Holtsville, NY, USA). Experiments were performed in triplicate.

The percentage encapsulation efficiency (%EE) and drug or dye loading (% DL), were evaluated by UV-Visible absorbance analysis by Nanodrop 2000c/2000 UV-Vis Spectrophotometers (Thermo scientific, Rockford, IL, USA). Briefly, 1 mg of RPV/Rho6G NPs and Rho6G NPs were dispersed in MQ water respectively. Further, the RPV (absorbance maximum at 306 nm¹⁵) and Rho6G (absorbance maximum at 535 nm¹⁶) loading concentrations in the NPs were estimated based on their respective standard curve. The %EE (Equation (1)) and % DL (Equation (2)) was estimated by the following formulas:

$$\%EE = \frac{\text{Amount of drug or dye loaded in the NP}}{\text{Starting amount of drug or dye}} \times 100 \quad (1)$$

$$\%DL = \frac{\text{Amount of drug or dye in the NPs}}{\text{Amount of polymer + drug or dye}} \times 100 \quad (2)$$

To evaluate the topography of the NPs, Scanning Electronic Microscope (SEM) imaging was performed. Briefly, the NPs suspension was filtered through a *Whatman*® Nuclepore Track-Etch Membrane (~ 50 nm pore size) and the membranes with the NPs were air dried, mounted to SEM stub, and sputter coated with a thin layer (~3-5 nm thick) of chromium. The samples were imaged under a Hitachi S-4700 Field-emission SEM (New York, NY, USA).

***In vitro* cellular uptake studies**

To evaluate cellular uptake in real time, HeLa cells (ATCC® CCL-2™) were cultured in RPMI-1640 medium with 10% FBS, 1 × L-Glutamine and 1 × Penstep solution. For all experiments the cells were cultured in a humidified incubator with 5 % CO₂ at 37°C at a density of 10⁵ cells/mL. To harvest these cells 1× Trypsin was used. All experiments were performed in triplicate. All the experiments were compared with untreated cells and free drug or dye treatments.

For *in vitro* concentration-dependent and time-dependent uptake studies, HeLa cells (10⁵ cells/mL) were seeded on 20×20 mm coverslips overnight (O/N). For concentration-dependent studies, Rho6G NPs were diluted in RPMI-1640 medium and the above coverslips with HeLa cells were treated at 5, 50, 500, and 5000 ng/mL concentrations respectively for 24 h. However, for time-dependent studies, above coverslips HeLa cells were treated with Rho6G NPs (at 500 ng/mL concentration) for 20 min, 1 h, 8 h, 16 h, 1 day, 2 days and 4 days. After respective treatment time period, cells were washed thrice with PBS before following plasma membrane stain with DiO dye as per manufacturer's protocol. After membrane staining, the cells were fixed with 4% PFA, followed by nuclear staining with Hoechst 33342 dye per manufacturer's protocol. Above cells were mounted by using Mowiol mounting medium. These cells were then analyzed by confocal imaging using Leica TCS SP8 MP multi-photon confocal microscope (Leica Microsystems Inc., Buffalo Grove, IL, USA), by using 40× Oil-objective (HC PL Apo, N.A. 1.30). The Hoechst 33342 stained nucleus was excited by using 405 nm laser, whereas DiO stained plasma membrane and Rho6G NPs were excited by 488 nm and 552 lasers unit. To improve the signal to noise ratio, 6 frames were averaged for each image. The images were taken at 512 × 512 eight-bit pixels. The images were processed with LAS X software (Leica Microsystems Inc., Buffalo Grove, IL, USA). The mean fluorescent intensity per cell was analyzed by LAS X software. Briefly, each cell area was specified and by using LAS X software the Rho6G intensity per cell was analyzed.

ARV drug intracellular release study by HPLC

To evaluate the intracellular release of ARV, 4ml (10⁵ cells/mL) of HeLa cells were treated with RPV/Rho6G NPs at different concentrations (50, 500, 5000 and 50000 ng/mL) for 24 h. After treatment the cells were trypsinised and washed three times with PBS. The cells were lysed with cell lysis

buffer (DMSO-PBS; 90% DMSO:10% PBS).¹⁷ After spinning down the cell lysate, the supernatant was collected and the amount of RPV drug as well as Rho6G dye release was qualified by HPLC analysis as previously described.¹⁸

The HPLC (Shimadzu, Columbia, Maryland, USA) instrument was equipped with LC-20AB pumps, SIL-20AC auto sampler and SPD-20A UV/Visible detector. The chromatographic separation was performed by Phenomenex® C-18 (150×4.6 mm, particle size 5 µm). The isocratic elution was performed by using a mixture of ACN to 25 mM KH₂PO₄ solution (55:45, v/v) where column was maintained at flow rate: 0.5 ml/min; temperature: 25°C; and detection: at 306 nm for RPV and 350 nm for Rho6G. The quantification was based on the area under the curve (AUC) analysis. The amount release was analyzed based on the standard curve analysis by HPLC. The instrument's inter-day and intra-day variability was <10 %. For correlation analysis of intracellular release between of Rho6G dye and RPV drug, data were obtained from 3 independent experiments and the mean ± standard error of means (SE) data were plotted to determine the intracellular release correlation between Rho6G dye and RPV drug from NPs.

Statistical Analysis

All experiments presented were performed in triplicate. In case of nanoparticle physiochemical analysis data are presented as the mean ± standard deviation (SD), whereas all cellular experiments were presented as the mean ± SE. For cellular experiments, data were analyzed by one-way analysis of variance (ANOVA) followed by post hoc (Bonferroni's multiple comparison test) and Pearson's correlation by using GraphPad Prism 5 software (La Jolla, CA, USA). The significant differences among treated and control groups at different concentration and overtime were considered to be statistically significant at $p < 0.05$. The *** and **** asterisk marks represents statistical significant at $p < 0.01$ and $p < 0.001$, respectively.

RESULT AND DISCUSSION

Characterization of NPs

The cARV drugs used in cART are mostly hydrophobic. This characteristic helps them to bind with HIV-1 enzymes inducing the formation of a hydrophobic pocket leading to inhibition of HIV-1 replication.⁴ However, this hydrophobic characteristic of ARV is the primary drawback causing poor tissue absorbability and short-systemic retention time. To enhance cARV drug uptake by cells, we propose the use of PLGA polymer based NPs as a drug carrier. PLGA polymer is a FDA recommended and well established polymer due to its biodegradable and controlled drug delivery potential.⁸ As a proof-of-concept for ARV loaded PLGA NPs formulation, we loaded rilpivirine (RPV) drug in the PLGA NPs. The RPV drug is a second-generation non-nucleoside reverse transcriptase inhibitor (NNRTI) that block HIV-viral genome transcription.^{19,20} Since RPV is a hydrophobic drug,⁴ o/w single emulsion solvent evaporation method was followed to ensure its potential encapsulation in the PLGA NPs (**Fig. 1**). Similarly, Rho6G dye or RPV/Rho6G uploaded PLGA NPs were also prepared by o/w emulsion method. The physiochemical characteristics of all the NPs are summarized in **Table I**.

TABLE I. PLGA NPs physiochemical characteristic estimation.

Type of PLGA NPs	Particle size (nm)	Zeta Potential (mV)	Polydispersity Index (PDI)	% EE	% DL
Rho6G NPs	106 ± 1.3	-27.69 ± 3.66	0.159 ± 0.019	22.7 ± 1.49	0.46 ± 0.02
RPV/Rho6G NPs	194 ± 2	-26.95 ± 0.85	0.120 ± 0.004	64.06 ± 0.09 ^a	8.00 ± 0.012 ^a
				13.7 ± 0.012 ^b	0.34 ± 0.0003 ^b

^aRilpivirine value;

^bRhodamine6G value; All data are presented as mean ± SD.

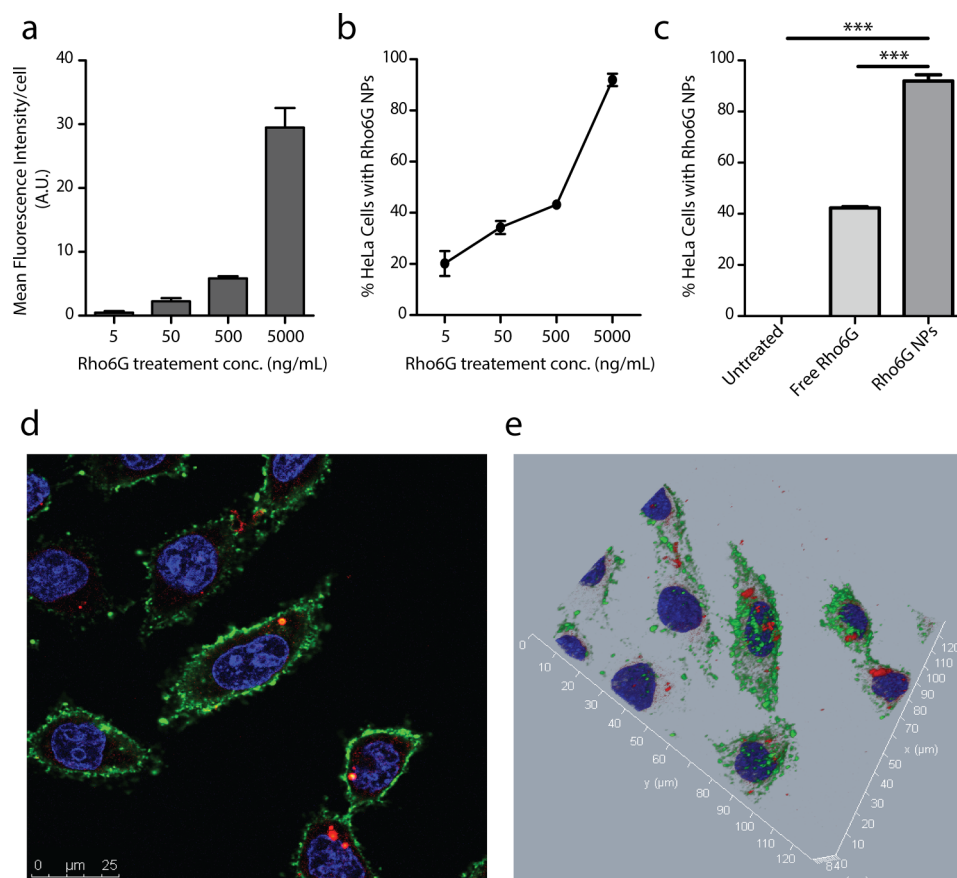


FIG. 2. Rho6G NPs treatment effect at different treatment concentrations. (a) Graph presents Mean Fluorescence Intensity (MFI) of Rho6G per cell after different Rho6G NPs treatment. (b) Graphical presentation of % of HeLa cells with Rho6G NPs after 24 h of treatment. (c) The graph presents Rho6G loading efficiency (% of HeLa cells loaded with Rho6G) Rho6G NPs treated cells in comparison to untreated and free Rho6G dye treated cells. For each experiment, an average of 100 cells were analyzed and data presents mean \pm SE of 3 independent experiments. The “***” asterisk mark represents statistical significant of $p < 0.001$. (d) Representative confocal fluorescence image showing HeLa cells loaded with Rho6G NPs after 24 h of treatment at 500 ng/mL. The cell nucleus, plasma membrane and Rho6G NPs are represented by the blue, green and red color respectively. (e) Represents the 3D view of figure 2(d) field, showing Rho6G NP (red) accumulation mostly near nucleus (blue).

The analysis shows that NP obtained by this method are $<200\text{nm}$ diameter and are narrow in size distribution. The SEM image reveals the NPs have uniform and smooth spherical surface (Fig. 1).

Although PLGA NPs can be prepared without the use of stabilizer, however we found⁹ and it has been reported by others²¹ that use of a stabilizer ensures particles stability, drug loading efficiency, and release characteristics. The use of 1 % PVA solution as aqueous phase and PF-127 as organic phase stabilizer results in enhanced drug loading, longer stability, and uniform size NPs.^{9,22} Thus the % EE of RPV and Rho6G in the same NP (RPV/Rho6G NPs), were calculated to be 64.06 ± 0.09 % and 13.7 ± 0.012 % respectively, whereas Rho6G NPs shows 22.7 ± 1.49 %. The encapsulation efficiency shows PLGA NP entrapment enhances the respective drug solubility when compared to free drug in aqueous medium ($< 0.1\text{g/L}$).²³

Confocal fluorescence Imaging

The advantage of using the multiphoton confocal fluorescence microscopic technique is that it enables proficient observation of fluorescent dye loaded NPs translocation and movement into the cells.²⁴ Therefore, to track the PLGA NPs in HeLa cells, Rho6G dye loaded NPs (Rho6G NPs) were

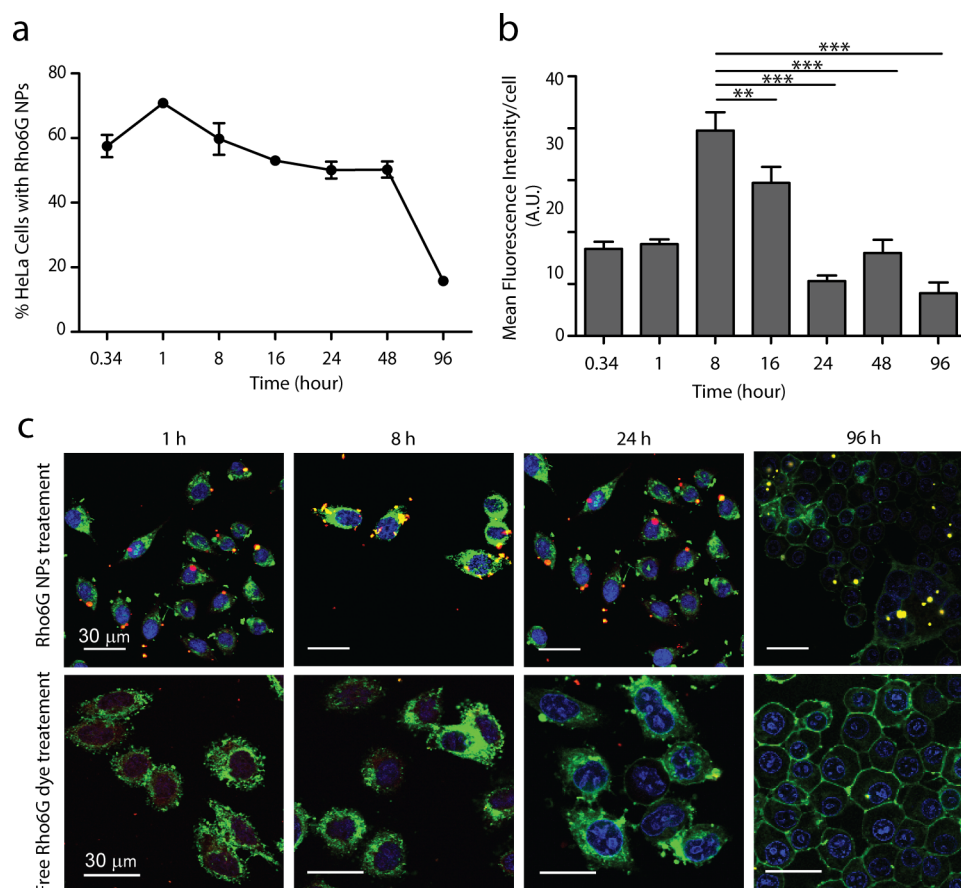


FIG. 3. Sustainability study of Rho6G NPs treatment over time. (a) Graphical presentation of % of cells with Rho6G NPs after 20 min (0.34 h), 1 h, 8 h, 16 h, 24 h, 48 h, and 96 h of treatment (at 500 ng/mL). (b) Graph presents Mean Fluorescence Intensity (MFI) of Rho6G per cell at different time point of Rho6G NPs treatment (at 500 ng/mL). For analysis, from each experiment on average 100 cells were analyzed and data presents mean \pm SE of 3 independent experiments. The ‘***’ and ‘****’ asterisk mark represent statistical significant of $p < 0.01$ and $p < 0.001$. (c) Representative confocal fluorescence image showing HeLa cells loaded with Rho6G NPs after different time point of treatment (at 500 ng/mL). First panel represents Rho6G NPs treated cell images and second panel represents free Rho6G dye treated cell image, over different time period. The color blue, green and red presents the cell nucleus, plasma membrane and Rho6G NPs or free Rho6G dye respectively.

formulated. In order to differentiate the nucleus and cytoplasm while observing cellular uptake of NPs, HeLa cells were stained with DiO (for plasma membrane²⁵) and Hoechst (for nucleus²⁶) dyes.

NP uptake and intracellular retention analysis

To investigate whether nano-encapsulation enhances drug uptake and retention in endothelial cells at the *in vitro* level, we used the HeLa cell line and compared the uptake efficiency with free Rho6G dye and Rho6G NPs at different concentrations over time. The HeLa cell line was chosen to mimic endothelial uptake,²⁷ which is the primary cell type that NPs encounter when administered subcutaneously (subQ) or intravenously (IV). Thus NP retention and drug release at the endothelial level primarily determines the efficacy of the ARV drug NP formulation.

To study Rho6G NP uptake efficiency, cells were incubated with different concentration of Rho6G NP (5, 50, 500, and 5000 ng/mL) and were also compared to free Rho6G dye at 5000 ng/mL for 24 h. The treated cells were evaluated for Rho6G uptake by confocal imaging utilizing the fluorescence property of Rho6G dye. The mean fluorescent intensity study per cell demonstrates that Rho6G dye nano-encapsulation enhances cellular Rho6G NPs uptake when compared to free Rho6G dye (Fig. 2(a) & 2(c)). Also, treatment at as low as 500 ng/mL Rho6G NPs shows that even after 24 h

of treatment ~45 % of the cells retains Rho6G NPs in their cytosol (**Fig. 2(b)**). Thus, these results support the hypothesis that nano-encapsulation potentially enhances ARV-drug uptake at the cellular level.

To determine Rho6G NPs adhesion on the cell membrane and their cellular distribution, the plasma membrane and nucleus were stained with DiO (green) and Hoechst (blue) (**Fig. 2(d) & 2(e)**). The Rho6G NPs were found to be mainly localized in the cytoplasm and around the nucleus. They have granular appearance and are mostly distributed in cytoplasm with almost none adherent at the cell membrane after 24 h of treatment (**Fig. 2(d) & 2(e)**). In contrast, free Rho6G dye shows continuous distribution throughout the cells, including the cell membrane, cytoplasm, and nucleus (**Fig. 3(c), lower panel**).

To evaluate the intracellular dye retention potential of the Rho6G NPs formulation, HeLa cells were treated with 500 ng/mL Rho6G NPs for 20 min, 1 h, 8 h, 16 h, 1 day, 2 day and 4 day (**Fig. 3**). The study shows, Rho6G NPs are retained within the cytoplasm for a significantly longer time than the free Rho6G dye (**Fig. 3(b) & 3(c)**). Moreover, the percent cell uptake study shows (**Fig. 3(b)**) that even on second day of treatment ~50 % of the cells retain the Rho6G NPs in the cytosol. Nonetheless, the Mean Fluorescence Intensity (MFI) study shows that the fluorescent intensity steadily diminishing, reflecting the slow intracellular release of Rho6G from the PLGA NPs encapsulation (**Fig. 3(b)**). The Rho6G NPs are mainly localized in the cytoplasm, around the nucleus and some even migrated to the nucleus over time (**Fig. 3(c)**). In contrast to Rho6G NPs, which are present even on the fourth day of treatment, the free Rho6G dye fades out within 1 day of treatment (**Fig. 3(c)**).

Intracellular drug release analysis

To verify whether and how much intracellular Rho6G dye release kinetics correlate with intracellular ARV-drug release from NPs, we performed HPLC analysis on cell-lysates from RPV/Rho6G NP treated HeLa cells. For this study, HeLa cells (10^5 cells/mL) were treated for 24 h with RPV/Rho6G NPs at different concentrations (50, 500, 5000, and 50000 ng/mL), respectively. After treatment, the cell membrane was dissolved using cell lysis buffer. The amount of Rho6G dye (absorbance at 350 nm) vs RPV drug (absorbance at 306 nm) in the cell lysate was then analyzed by HPLC. **Figure 4** shows the correlation analysis between Rho6G dye and RPV drug release pattern. The positive Pearson's 'r' correlation value, demonstrates that amount of intracellular Rho6G release is positively and significantly correlated with RPV release Rho6G dye release profile from nano-encapsulation. Thus, this

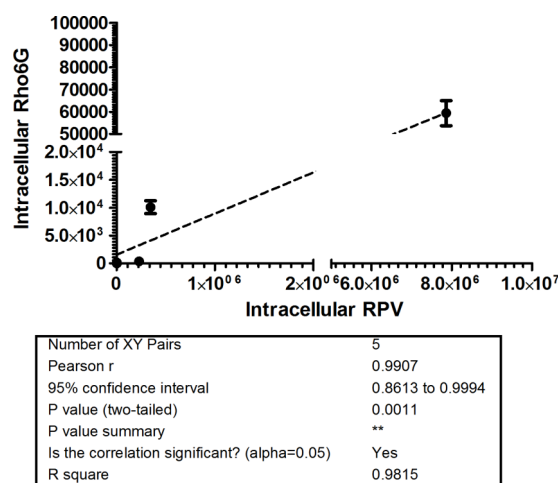


FIG. 4. Correlation between intracellular release of Rho6G dye and RPV drug from NPs at different treatment concentration (50, 500, 5000, and 50000 ng/mL). Each data presents mean \pm SE of 3 independent experiments. The box below the graph presents the Pearson's 'r' correlation value and corresponding P-value. The data represented means \pm SE of 3 independent experiments. The *** asterisk mark represent statistical significant of $p < 0.01$.

study verifies our assumption that Rho6G dye release kinetics from Rho6G NPs mimics the RPV drug release profile from RPV NPs.

In this present study, the use of ultra-sensitive confocal fluorescent microscope has enabled us to evaluate the sustained drug delivery potential of the ARV drug loaded PLGA NPs. The NPs were formulated by using o/w emulsification method. The physicochemical properties analysis (Table I) revealed that PLGA-NPs show enhanced ARV drug loading efficiency. The confocal fluorescence microscopic studies clearly demonstrate the pharmacokinetic properties of NPs uptake and sustained drug release, at the cellular level. Present experimental analysis demonstrates the Rho6G dye release profile from nano-encapsulation and supports our hypothesis that PLGA NP enhances ARV drug entrapment; cellular uptake, retention and sustained release of drug. Furthermore, this formulation also endorses the potential of PLGA NPs to further improve the *in-vivo* efficacy of cARV drug. Our study also indicates that confocal microscopic studies have enormous potential to evaluate nano-drug delivery mechanisms at the cellular level. Further, ARV drug-loaded PLGA NPs provide a platform for development of new and improved nano-drug delivery systems to promote cART adherence for HIV/AIDS treatment and prevention, opening new frontiers in the field of HIV/AIDS translational research.

ACKNOWLEDGEMENTS

This project and publication were funded by NIAID R01AI117740-01, 2015 (to C.J.D.) and NI-AID 1 R15AI118550-01, 2015, (to A.S.) project awards. The authors would like to acknowledge the Integrated Biomedical Imaging Facility, Department of Biomedical Sciences, Creighton University School of Medicine for allowing us to use the confocal core facility.

- ¹ R. Yuste, *Nature methods* **2**(12), 902-904 (2005).
- ² L. Shang, K. Nienhaus, X. Jiang, L. Yang, K. Landfester, V. Mailander, T. Simmet, and G. U. Nienhaus, *Beilstein journal of nanotechnology* **5**, 2388-2397 (2014).
- ³ WHO, 2007.
- ⁴ E. J. Arts and D. J. Hazuda, *Cold Spring Harbor perspectives in medicine* **2**(4), a007161 (2012).
- ⁵ D. S. Fierer and M. E. Klotman, *Current opinion in HIV and AIDS* **1**(2), 115-120 (2006).
- ⁶ T. W. Chun, D. C. Nickle, J. S. Justement, J. H. Meyers, G. Roby, C. W. Hallahan, S. Kottitil, S. Moir, J. M. Mican, J. I. Mullins, D. J. Ward, J. A. Kovacs, P. J. Mannon, and A. S. Fauci, *The Journal of infectious diseases* **197**(5), 714-720 (2008).
- ⁷ M. Horiike, S. Iwami, M. Kodama, A. Sato, Y. Watanabe, M. Yasui, Y. Ishida, T. Kobayashi, T. Miura, and T. Igarashi, *Virology* **423**(2), 107-118 (2012).
- ⁸ H. K. Makadia and S. J. Siegel, *Polymers* **3**(3), 1377-1397 (2011).
- ⁹ C. J. Destache, T. Belgum, M. Goede, A. Shibata, and M. A. Belshan, *The Journal of antimicrobial chemotherapy* **65**(10), 2183-2187 (2010).
- ¹⁰ G. Sahay, D. Y. Alakhova, and A. V. Kabanov, *Journal of controlled release : official journal of the Controlled Release Society* **145**(3), 182-195 (2010).
- ¹¹ T. Bose, D. Latawiec, P. P. Mondal, and S. Mandal, *Journal of Nanoparticle Research* **16**(8), 1-25 (2014).
- ¹² L. Shang, K. Nienhaus, and G. U. Nienhaus, *Journal of Nanobiotechnology* **12**(5), (2014).
- ¹³ H. Fessi, F. Puisieux, J. P. Devissaguet, N. Ammoury, and S. Benita, *International Journal of Pharmaceutics* **55**(1), R1-R4 (1989).
- ¹⁴ R. L. McCall and R. W. Sirianni, *Journal of visualized experiments : JoVE* (82), 51015 (2013).
- ¹⁵ R. Vijayalakshmi, Vadapalli S. H. Naveena, J. Philip, and M. D. Dhanaraju, *Der Pharma Chemica* **6**(1), 404-406 (2014).
- ¹⁶ S. Ghosh, A. Roy, D. Banik, N. Kundu, J. Kuchlyan, A. Dhir, and N. Sarkar, *Langmuir : the ACS journal of surfaces and colloids* **31**(8), 2310-2320 (2015).
- ¹⁷ G. Wang, Y. Gong, F. J. Burczynski, and B. B. Hasinoff, *Free radical research* **42**(5), 435-441 (2008).
- ¹⁸ A. A. Date, A. Shibata, P. Bruck, and C. J. Destache, *Biomedical chromatography : BMC* **29**(5), 709-715 (2015).
- ¹⁹ D. Ripamonti and F. Maggiolo, *Current opinion in investigational drugs (London, England : 2000)* **9**(8), 899-912 (2008).
- ²⁰ G. J. Zaharatos and M. A. Wainberg, *Annals of medicine* **45**(3), 236-241 (2013).
- ²¹ F. Danhier, N. Lecouturier, B. Vroman, C. Jerome, J. Marchand-Brynaert, O. Feron, and V. Preat, *Journal of controlled release : official journal of the Controlled Release Society* **133**(1), 11-17 (2009).
- ²² M. M. Yallapu, B. K. Gupta, M. Jaggi, and S. C. Chauhan, *Journal of colloid and interface science* **351**(1), 19-29 (2010).
- ²³ D. Lawrence, B. Sanders, and O. K. Sharma, in *NIH AIDS Reagent Program, Beerse, Belgium* (2014).
- ²⁴ P. P. Mondal and A. Diaspro, in *Fundamentals of Fluorescence Microscopy*, edited by P. P. Mondal and A. Diaspro (Springer, 2014), Vol. 1, pp. 149-159.
- ²⁵ J. A. Ankrum, O. R. Miranda, K. S. Ng, D. Sarkar, C. Xu, and J. M. Karp, *Nature protocols* **9**(2), 233-245 (2014).
- ²⁶ A. Bloom and N. Winograd, *Surface and interface analysis : SIA* **46**(Suppl 1), 177-180 (2014).
- ²⁷ R. Agarwal, V. Singh, P. Jurney, L. Shi, S. V. Sreenivasan, and K. Roy, *Proceedings of the National Academy of Sciences of the United States of America* **110**(43), 17247-17252 (2013).